1. Supporting figures

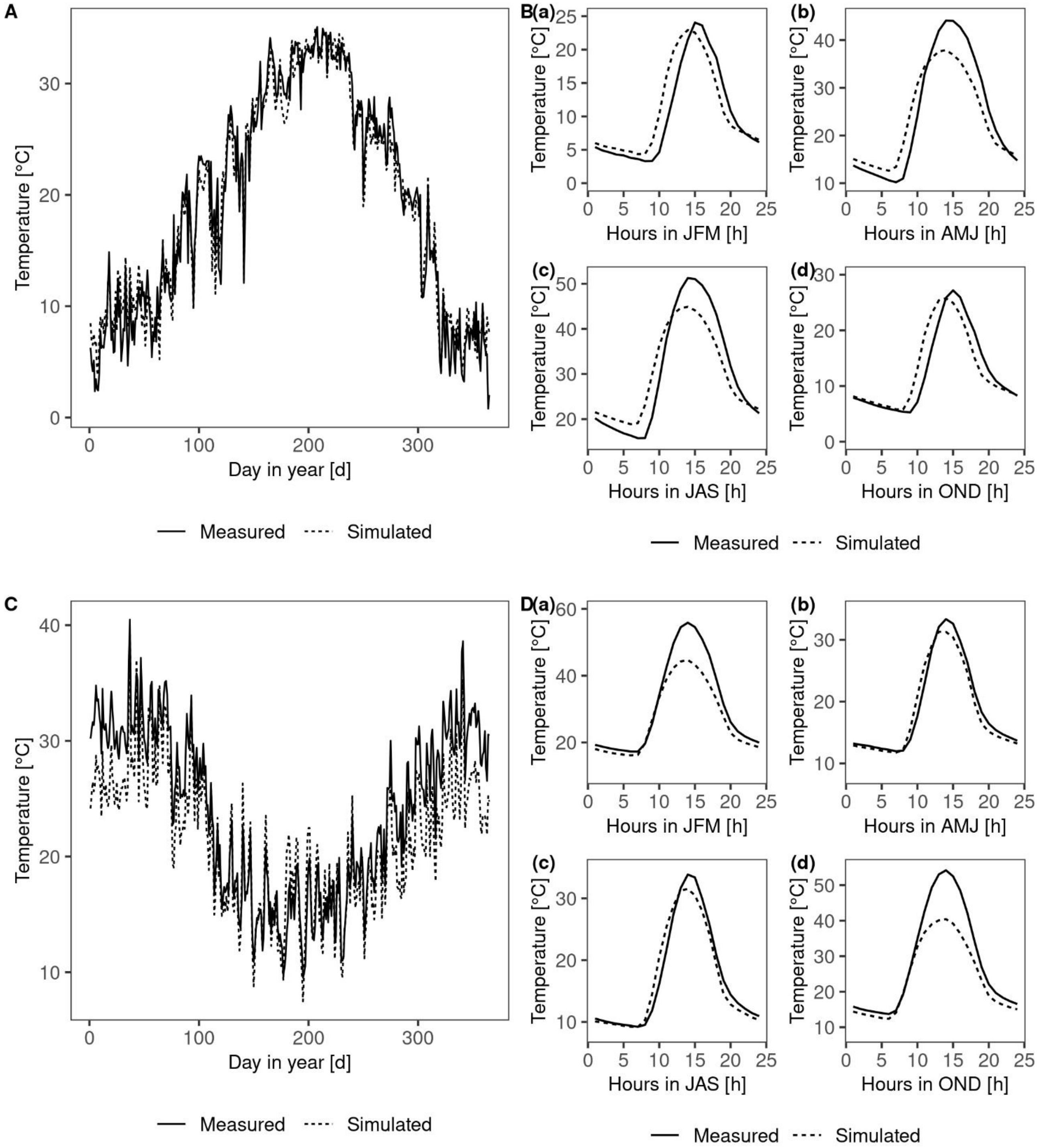

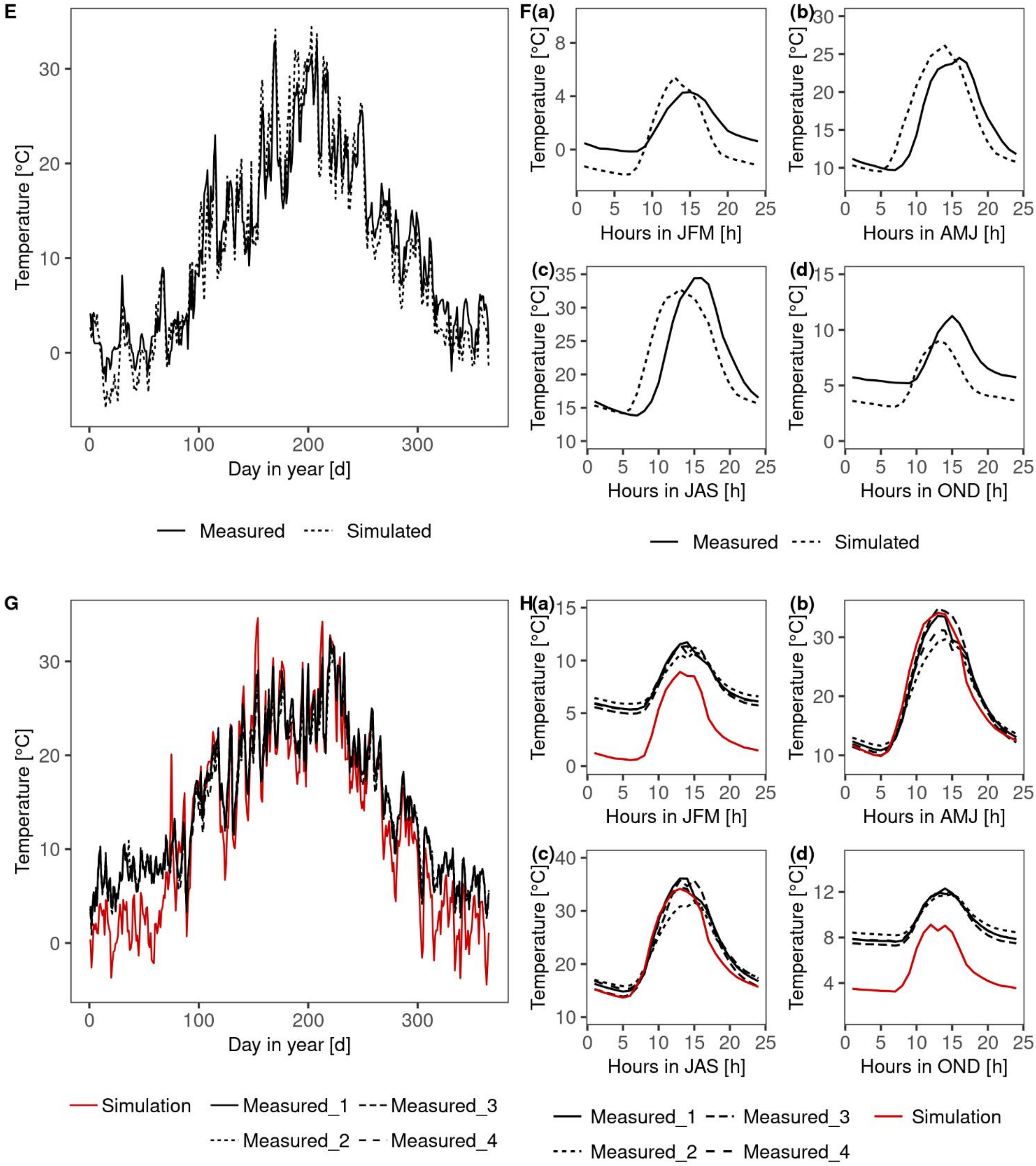
E
Temperature [°C]
Day in year [d]
Measured
Simulated
F(a)
Hours in JFM [h]
(b)
Hours in AMJ [h]
(c)
Hours in JAS [h]
(d)
Hours in OND [h]
G
Simulation
Measured_1
Measured_2
Measured_3
Measured_4
H(a)

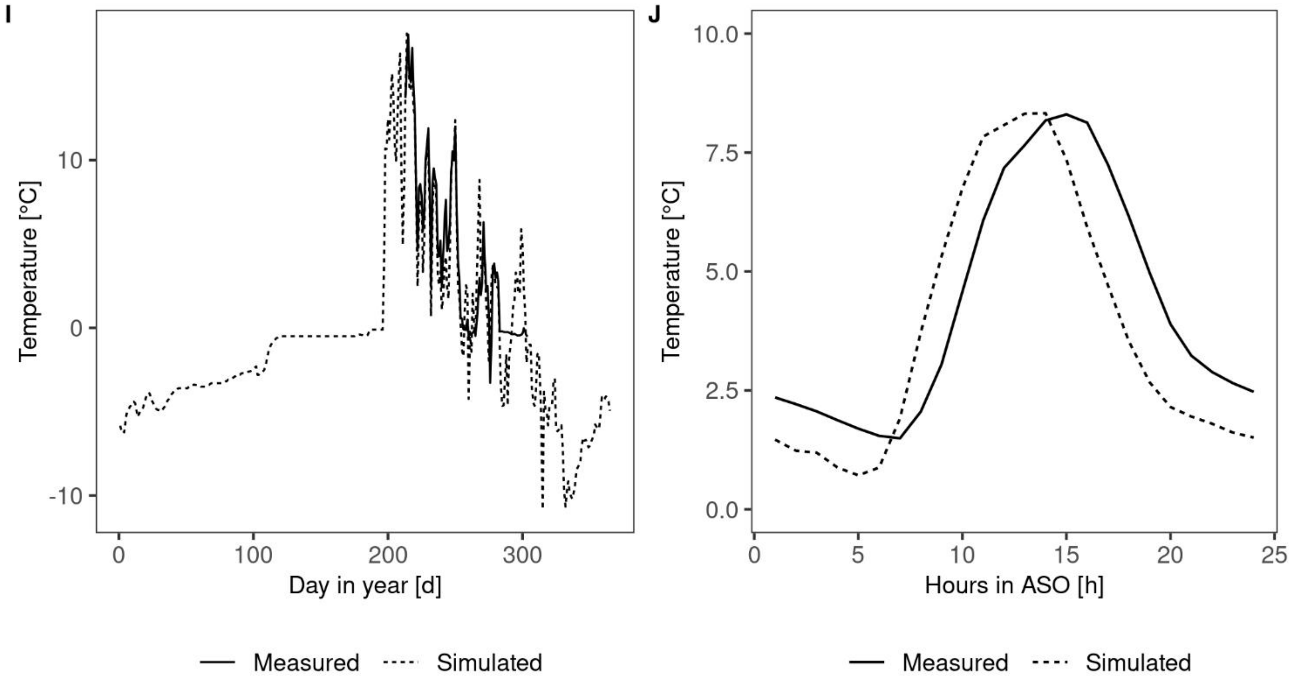

Figure S1: Calibration of abiotic parameters for the data-driven model via comparing the seasonal (left panel) and diurnal (right panel) surface temperature of lichen-dominated species at sites D1 (A, B), D2 (C, D), T1 (E, F), T3 (G, H) and A1 (I, J); at site T3 the simulated patterns of moss-dominated species was compared to measured temperature data by four sensors at different locations. In the right panel describing the diurnal patterns, the (a), (b), (c) and (d) indicate the comparison of patterns of hourly average data in January, February and March (JFM); April, May and June (AMJ); July, August and September (JAS); October, November and December (OND), respectively. At site A1, the average data was during August, September and October (ASO).

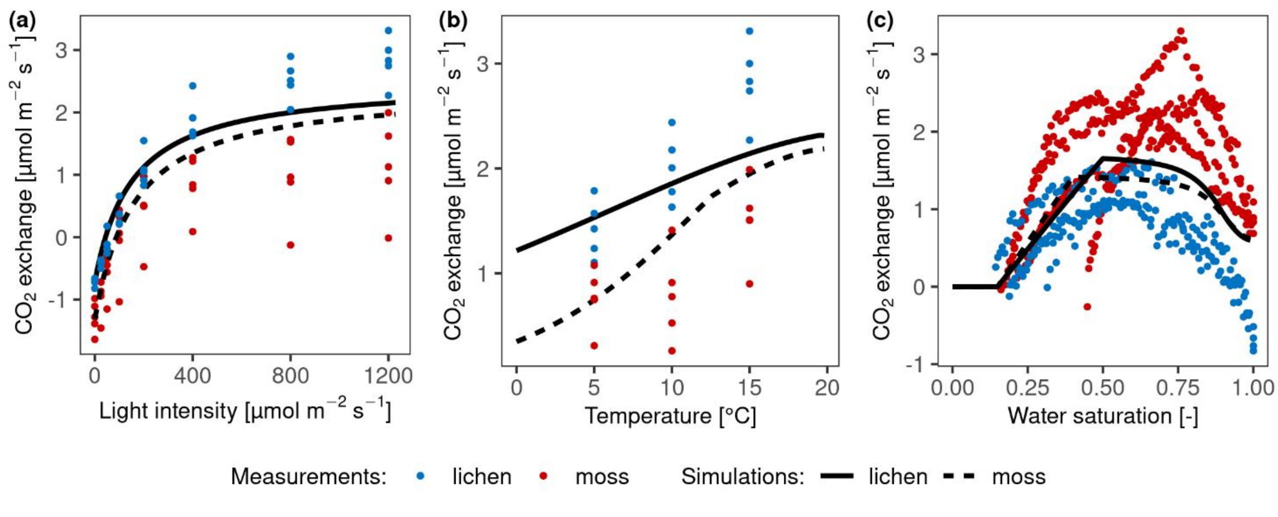

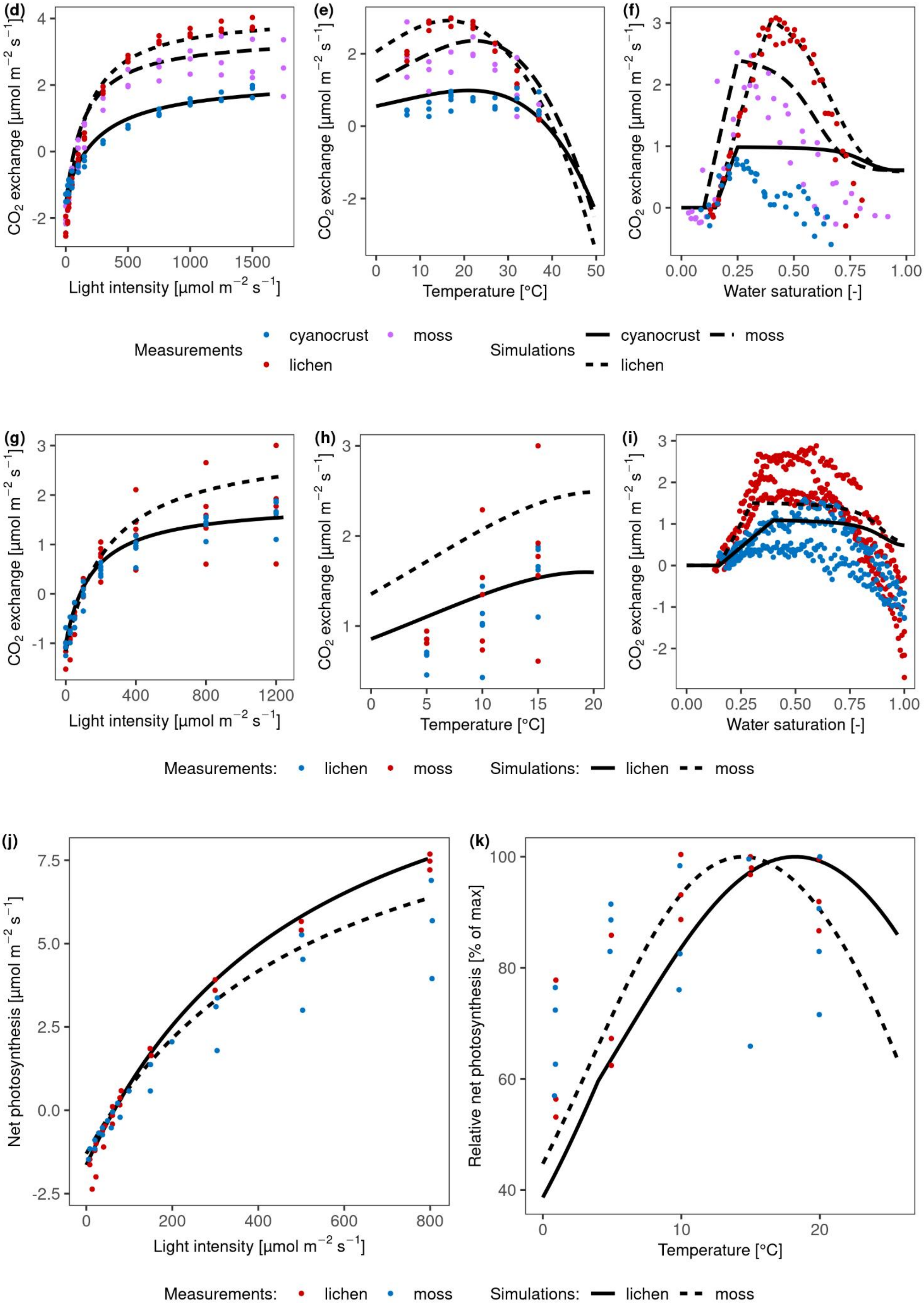
(d)
(e)
(f)
CO2 exchange [µmol m−2 s−1]
Light intensity [µmol m−2 s−1]
Temperature [°C]
Water saturation [-]
Measurements
cyanocrust
moss
lichen
Simulations
cyanocrust
moss
lichen
(g)
(h)
(i)
CO2 exchange [µmol m−2 s−1]
Light intensity [µmol m−2 s−1]
Temperature [°C]
Water saturation [-]
Measurements:
lichen
moss
Simulations:
lichen
moss
(j)
(k)
Net photosynthesis [µmol m−2 s−1]
Relative net photosynthesis [% of max]
Light intensity [µmol m−2 s−1]
Temperature [°C]
Measurements:
lichen
moss
Simulations:
lichen
moss

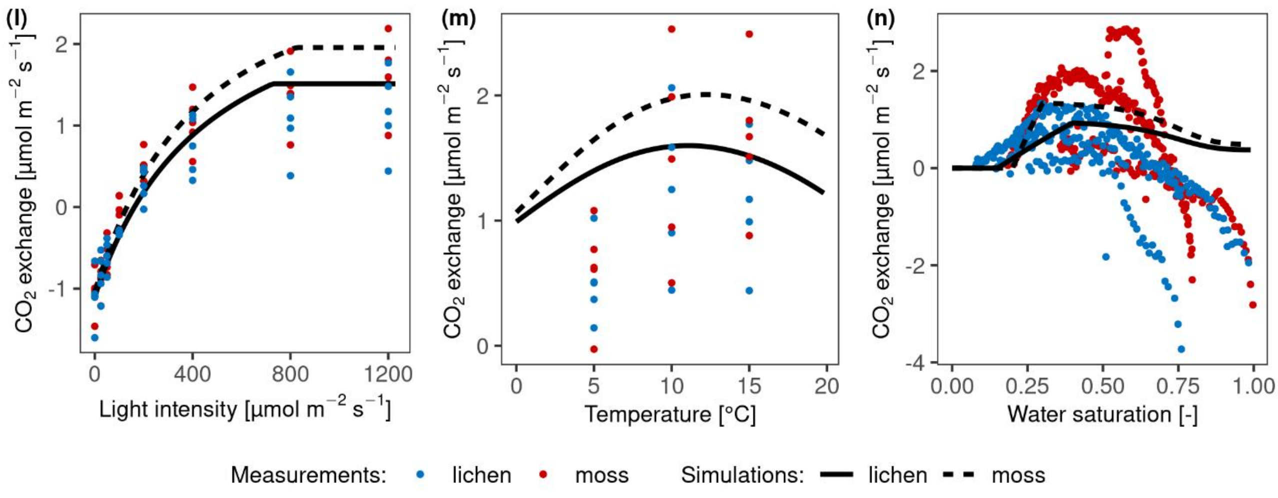

Figure S2: Calibration results of physiological traits for the data-driven model at site D1 (a, b, c), D2 (d, e, f), T1 (g, h, i), T3 (j, k) and A1 (l, m, n), via fitting the photosynthetic response curves to some environmental factors. (a, d, g, j, l): net photosynthesis rate in response to light at optimum water content (OWC) and 15°C at D1, T1 and A1; OWC and 22 °C at D2; water saturation for 30% and 15°C at T3. (b, e, h, k, m): net photosynthesis rate in response to temperature at 1200 µmol m^{-2} s^{-1} light and OWC at D1, T1 and A1; 500 µmol m^{-2} s^{-1} light and OWC at D2; 1500 µmol m^{-2} s^{-1} light and water saturation for 30% at T3. (c, f, i, n): net photosynthesis rate in response to relative water saturation at 400 µmol m^{-2} s^{-1} light and 15°C at D1, T2 and A1; 500 µmol m^{-2} s^{-1} light and 22 °C at D2.

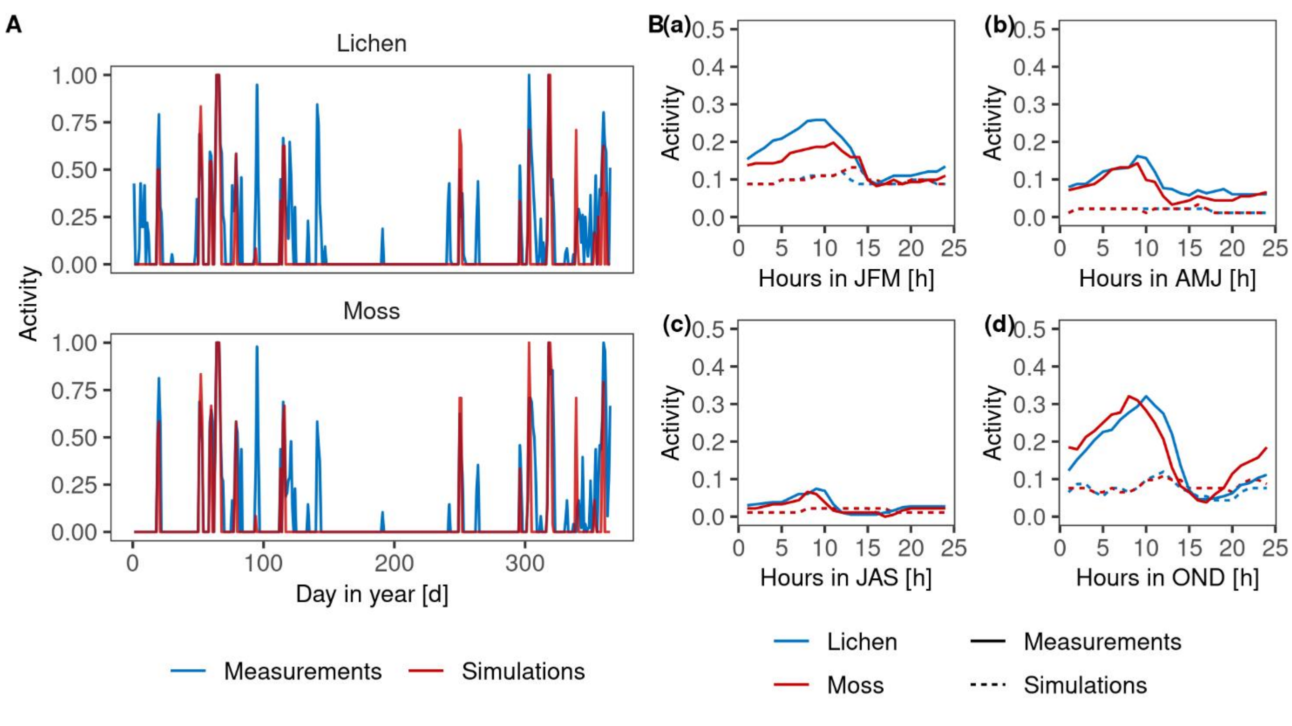

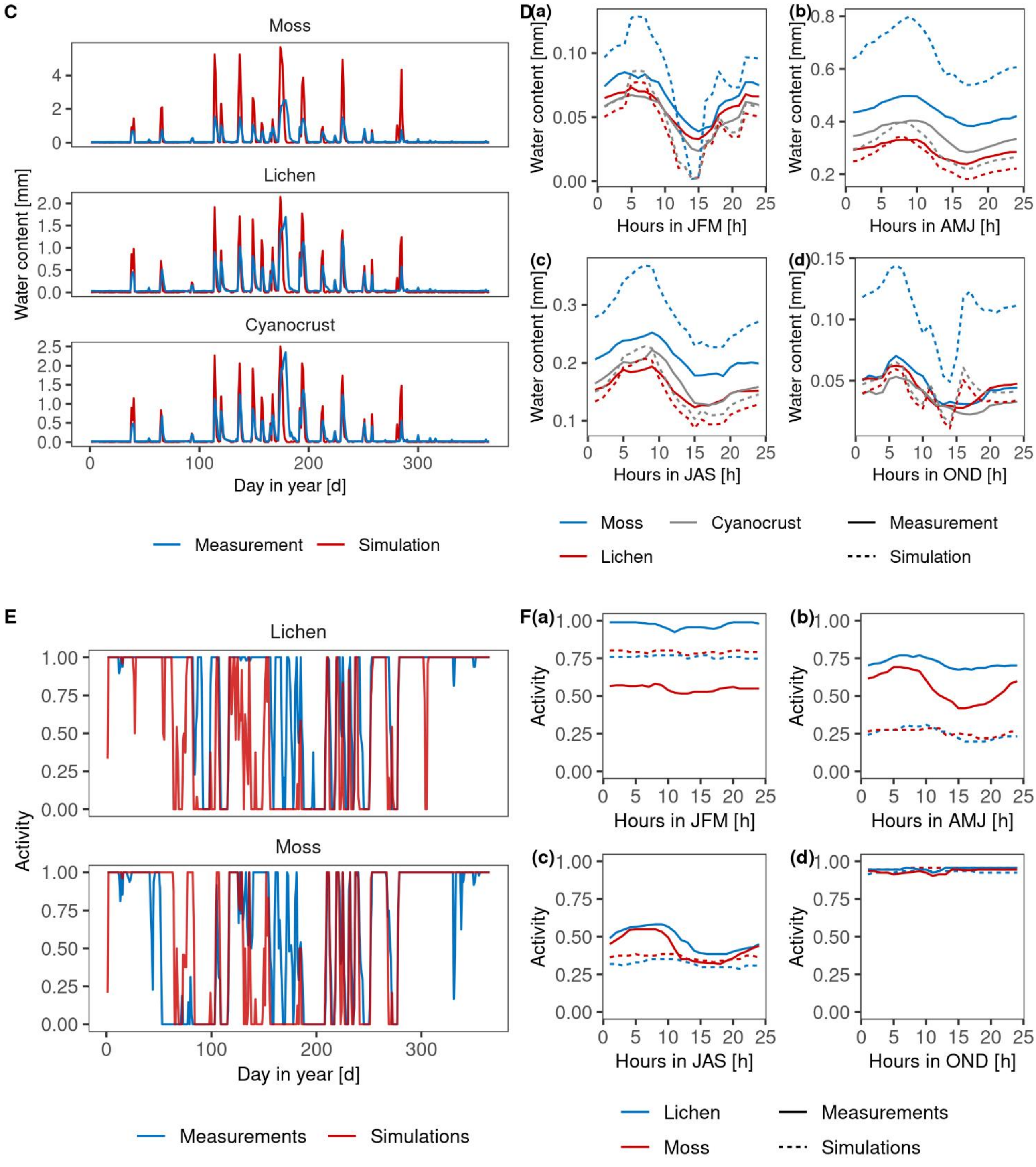
C
Moss
Lichen
Cyanocrust
Water content [mm]
Day in year [d]
Measurement
Simulation
D(a)
(b)
(c)
(d)
Water content [mm]
Hours in JFM [h]
Hours in AMJ [h]
Hours in JAS [h]
Hours in OND [h]
Moss
Cyanocrust
Measurement
Lichen
Simulation
E
Lichen
Moss
Activity
Day in year [d]
Measurements
Simulations
F(a)
(b)
(c)
(d)
Activity
Hours in JFM [h]
Hours in AMJ [h]
Hours in JAS [h]
Hours in OND [h]
Lichen
Measurements
Moss
Simulations

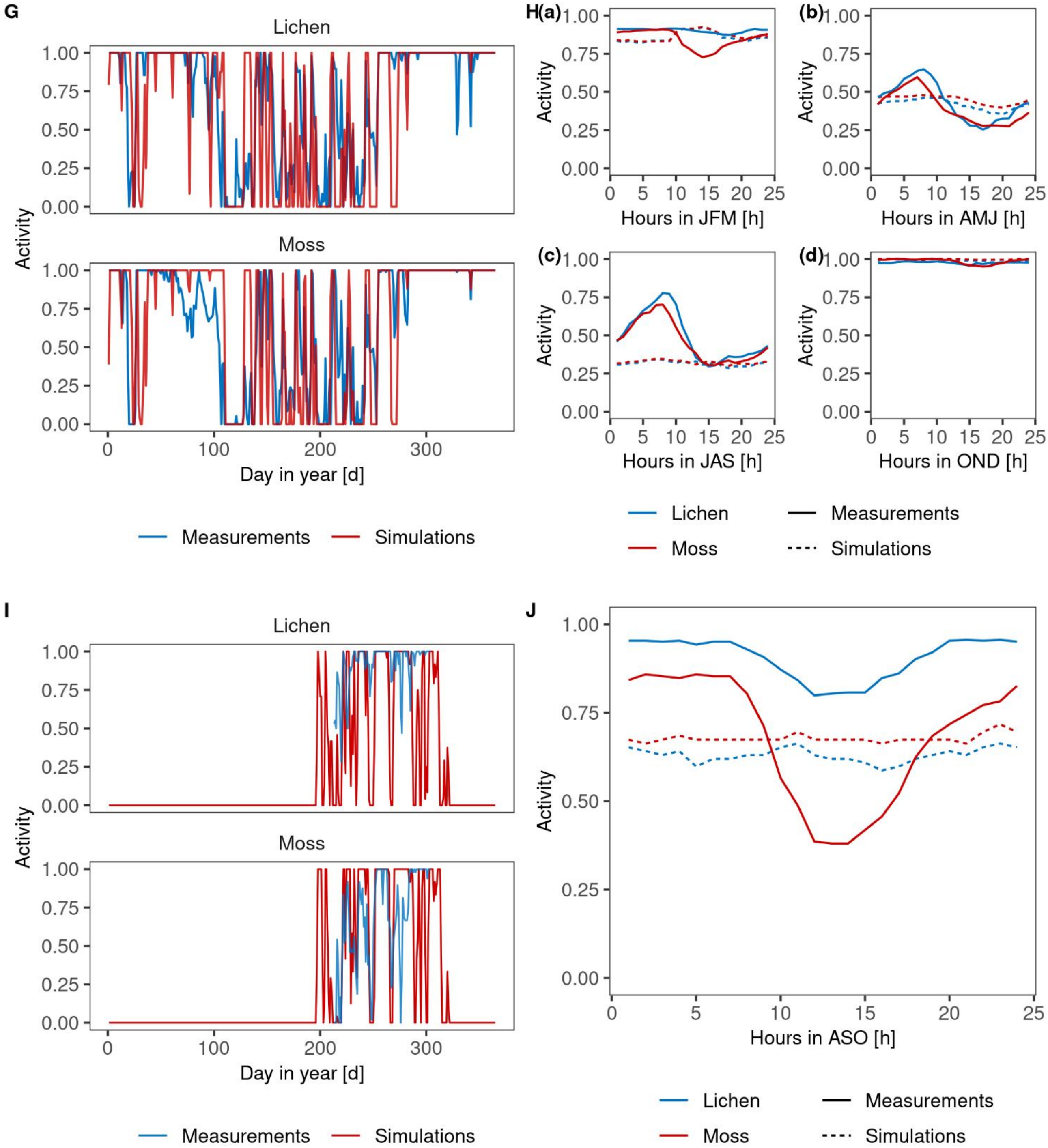

Figure S3: Validation of the water and energy balance in the data-driven model via comparing the seasonal (left panel) and diurnal (right panel) water content at site D2 (C, D) or activity patterns of lichen- and moss-dominated species at sites D1 (A, B), T1 (E, F), T2 (G, H) and A1 (I, J); at site T3 the simulated patterns of activity was compared to measured data by four sensors at different locations. In the right panel describing the diurnal patterns, the (a), (b), (c) and (d) indicate the comparison of the hourly average data in January, February and March (JFM); April, May and June (AMJ); July, August and September (JAS); October, November and December (OND), respectively. At site A1, the average data was during August, September and October (ASO).

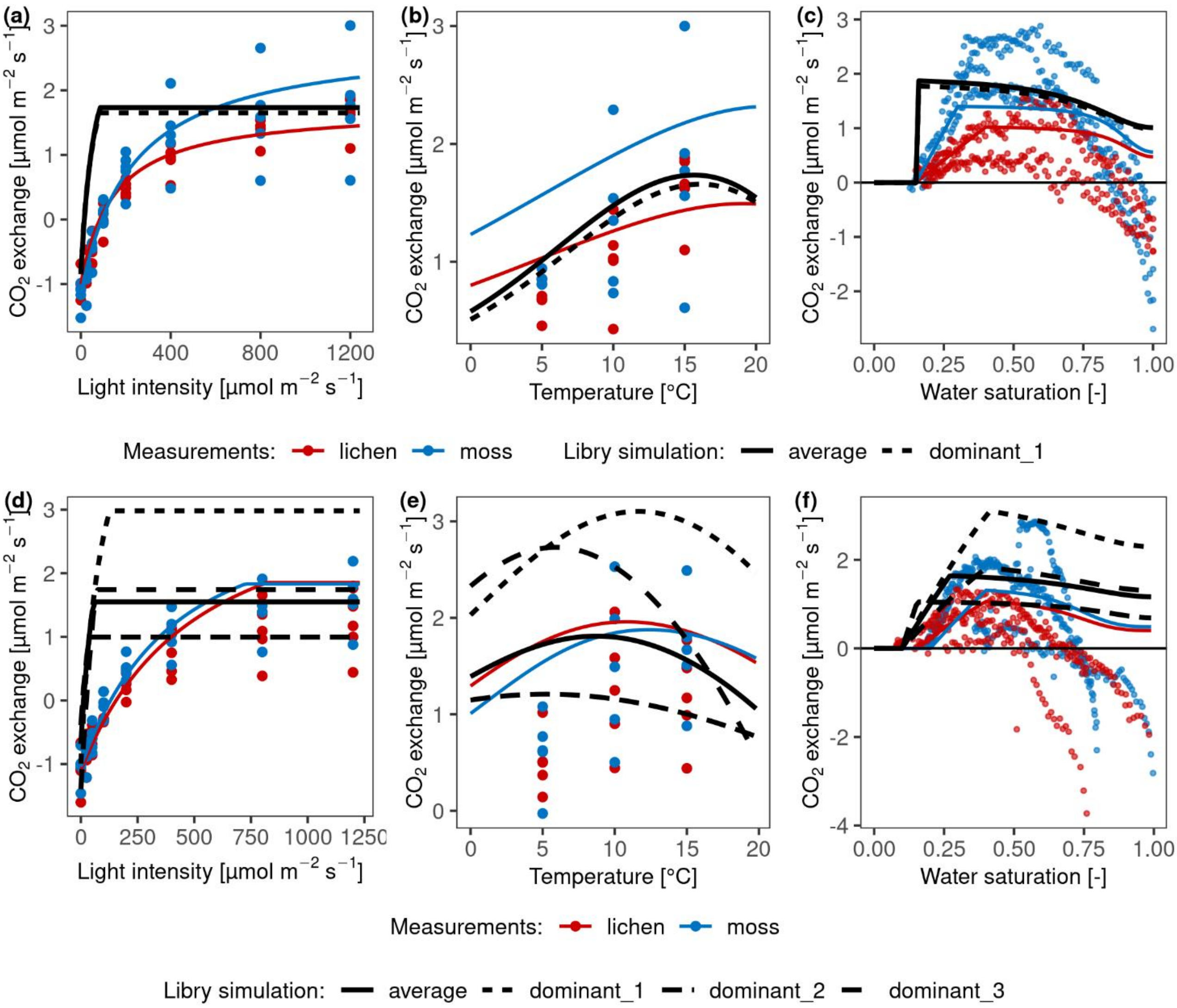

Figure S4: Comparison of photosynthetic performance of dominant strategies selected by LiBry model and the measured data as well as the fitted response curves by data-driven model in site T1 (a, b, c) and A1 (d, e, f). (a, d): photosynthesis relation in response to light intensity; (b, e): photosynthesis relation in response to temperature; (c, f): photosynthesis relation in response to water saturation. The colored points and lines represent the measured and simulated by data-driven model CO_2 exchange rates of moss and lichens. The black lines show the simulated photosynthetic relations of the most dominant strategies with positive C balance selected by LiBry model and the average strategy calculated by LiBry model. The parameter values for the average strategy are the average of the corresponding parameters for all selected surviving strategies.

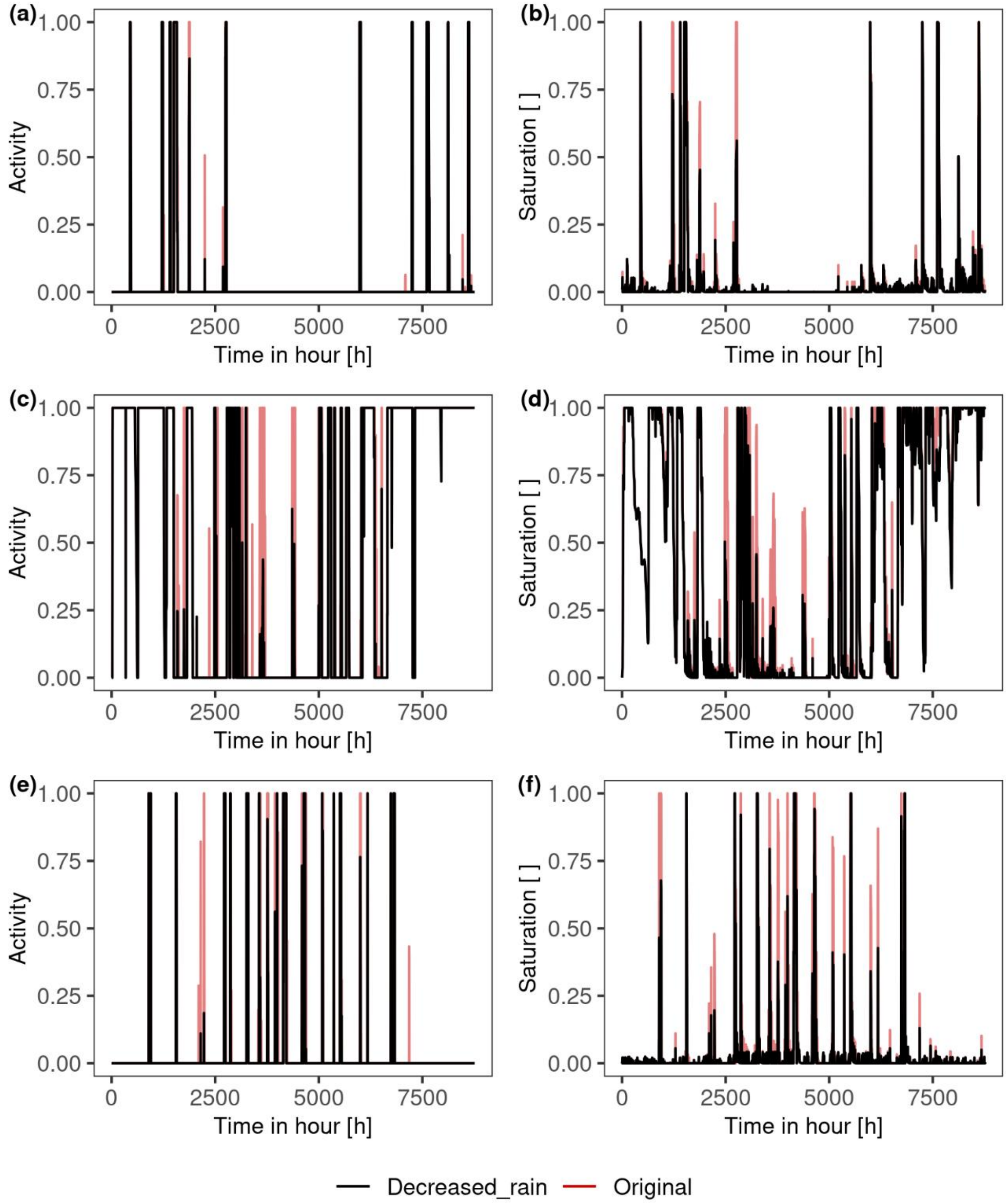

Figure S5: Comparison of simulated hourly activity and relative water saturation of lichen-dominated species at site D1 (a and b), T1 (c and d) and D2 (e and f) between original rainfall amount and reduced rainfall by half. Black lines represent the patterns when input rainfall amount decreases by half for each rainfall event, red lines represent the patterns when the input rainfall maintains consistency with measured.

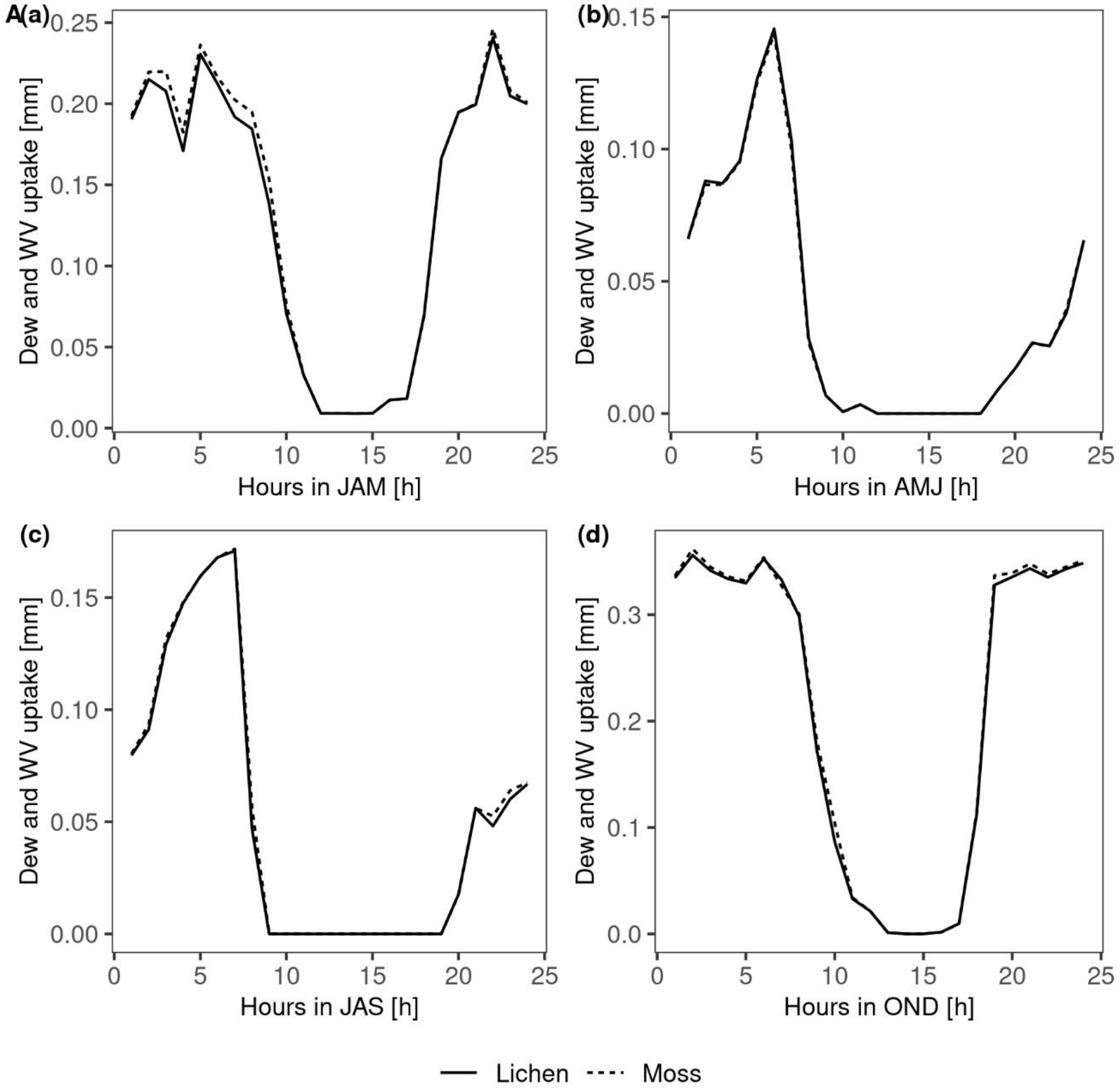
A(a)
Dew and WV uptake [mm]
Hours in JAM [h]
(b)
Hours in AMJ [h]
(c)
Hours in JAS [h]
(d)
Hours in OND [h]
Lichen
Moss

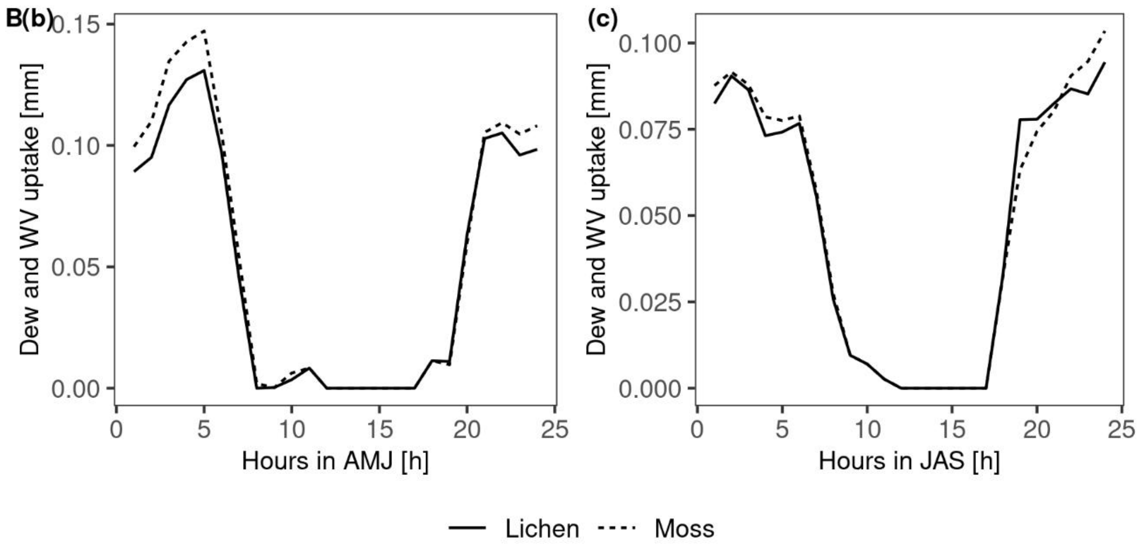
B(b)
Dew and WV uptake [mm]
Hours in AMJ [h]
(c)
Hours in JAS [h]
Lichen
Moss

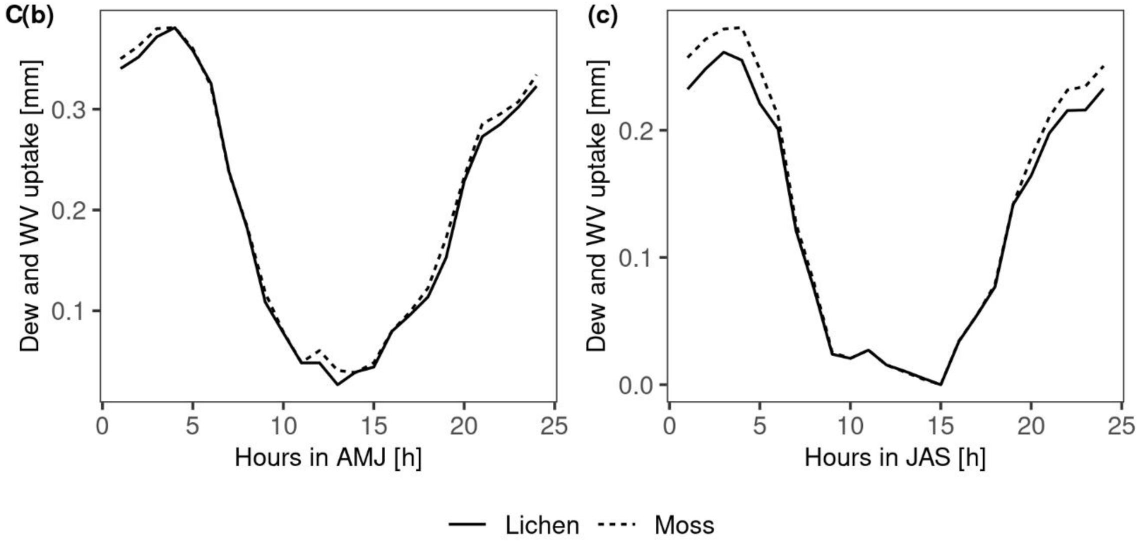

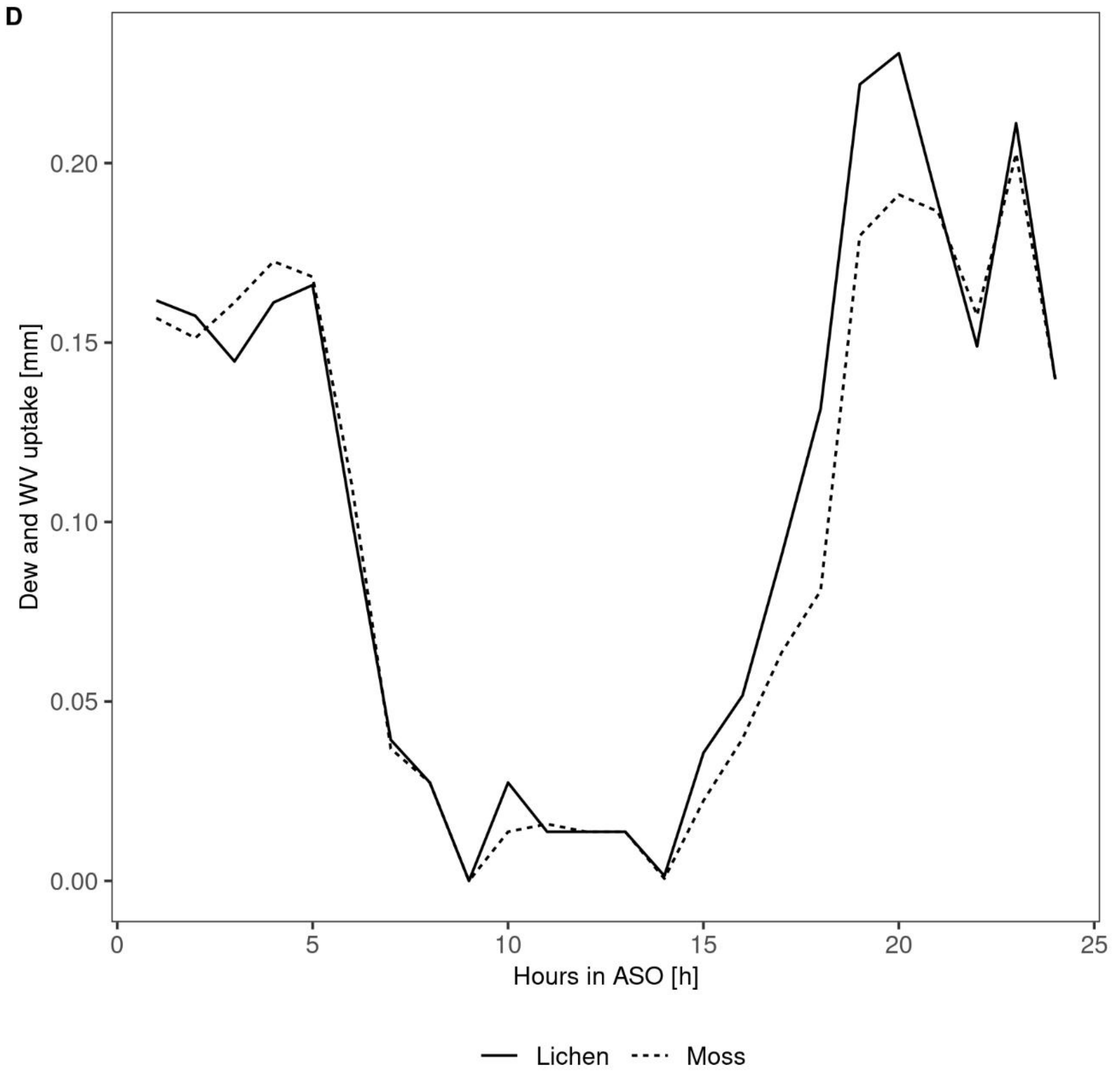

Figure S6: Modeled hourly sum of dew and water vapor uptake of lichen- and moss-dominated biocrusts at site D1 (A), T1 (B), T2 (C) and A1 (D) during seasons when an obvious underestimation of activity at night and morning can be observed. (a): diurnal pattern during the period January, February and March (JFM); (b): diurnal pattern during the period April, May and June (AMJ); (c): diurnal pattern during the period July, August and September (JAS); (d): diurnal pattern during the period October, November and December (OND); ASO represents August, September and October.

2. Details about the LiBry model

LiBry model was used to simulate the dynamics of non-vascular vegetation (including lichens, bryophytes, and cyanobacteria) at various research sites (Porada et al., 2013, 2014, 2017, 2018; Porada and Giordani, 2021). The LiBry model select strategies with optimal values for functional traits, adapting to the predefined climatic conditions. The physiological and morphological parameters of each strategy are photosynthetic capacity, thallus specific area, etc. The value of each parameter is randomly generated from their respective possible ranges, which are derived from the literature, with trait combinations subject to biophysical and physiological constraints/trade-offs (see Porada et al., 2013).

The model is driven by a time series of climatic forcing data and other abiotic parameters describing the habitat, such as disturbance interval, the surface roughness length, etc. Some of the abiotic parameters can be derived more easily by calibration. Parameters like roughness length, soil thermal conductivity, or soil heat capacity, for instance, are calibrated through the fitting of model equations concerning water and energy fluxes to daily and diurnal patterns of measured surface temperature and moisture. A large number of strategies with combinations of the different parameter values are generated by the model before the start of the simulation. The carbon dynamics of each strategy is calculated based on physiological and biochemical mechanisms. For example, an organism gains carbon through photosynthesis and releases it by respiration. The gross photosynthesis rate is calculated based on the Farquhar photosynthesis scheme (Farquhar and von Caemmerer, 1982); respiration is temperature-dependent (Q10 relationship).

C balance then translates into biomass, resulting in growth in cover if this translated biomass is larger than the biomass lost due to tissue turnover, whereas a negative C balance, as well as disturbance, leads to mortality, and thus a shrinkage of the cover. In the end, the strategies that have a positive cover area in the long term survive in the model. In other words, the survival of strategies is determined by their C balance.

The LiBry model ran for 300 years to simulate the dynamics of generated 1000 strategies. The input of such a large number of strategies is to ensure that the combinations of all possible values of all functional traits in research sites are considered for selection by the LiBry model.

3. References

Farquhar, G. D. and von Caemmerer, S.: Modelling of Photosynthetic Response to Environmental Conditions, in Physiological Plant Ecology II, edited by O. L. Lange, pp. 549–587, Springer, Berlin, Heidelberg., 1982.

Porada, P. and Paolo, G.: Bark Water Storage Plays Key Role for Growth of Mediterranean Epiphytic Bark Water Storage Plays Key Role for Growth of Mediterranean Epiphytic Lichens, Front. For. Glob. Chang., 4, 30, doi:10.3389/ffgc.2021.668682, 2021.

Porada, P., Weber, B., Elbert, W., Pöschl, U. and Kleidon, A.: Estimating global carbon uptake by lichens and bryophytes with a process-based model, Biogeosciences, 10, 6989–7033, doi:10.5194/bg-10-6989-2013, 2013.

Porada, P., Weber, B., Elbert, W., Pöschl, U. and Kleidon, A.: Estimating impacts of lichens and bryophytes on global biogeochemical cycles, Global Biogeochem. Cycles, 28(2), 71–85, doi:10.1002/2013GB004705.Received, 2014.

Porada, P., Pöschl, U., Kleidon, A., Beer, C. and Weber, B.: Estimating global nitrous oxide emissions by lichens and bryophytes with a process-based productivity model, Biogeosciences, 14, 1593–1602, doi:10.5194/bg-14-1593-2017, 2017.

Porada, P., Van Stan II, J. T. and Kleidon, A.: vegetation to global rainfall interception, Nat. Geosci., 11, 563–567, doi:10.1038/s41561-018-0176-7, 2018.